

Magnetic field controlled electron transport in a thin cylinder

Santanu K. Maiti^{1,2}

¹Theoretical Condensed Matter Physics Division, Saha Institute of Nuclear Physics,
1/AF, Bidhannagar, Kolkata-700 064, India

²Department of Physics, Narasinha Dutt College, 129, Belilious Road, Howrah-711 101, India

Abstract

We explore electron transport in a thin cylinder, attached to two semi-infinite one-dimensional metallic electrodes, in the presence of both longitudinal and transverse magnetic fluxes. A simple tight-binding model is used to describe the system, where all the calculations are performed in the Green's function formalism. Quite surprisingly it is observed that, typical current amplitude oscillates as a function of the transverse magnetic flux, associated with conductance-energy characteristics, showing $N \phi_0$ flux-quantum periodicity, where N and ϕ_0 ($= \hbar c/e$) correspond to the system size and elementary flux-quantum respectively. The analysis might be helpful in fabricating mesoscopic switching devices, where a particular response can be delayed by tuning the system size N .

PACS No.: 73.63.Fg; 73.63.Rt.

Keywords: Thin cylinder; Conductance; I-V characteristic; Radial magnetic field.

Corresponding Author: Santanu K. Maiti
Electronic mail: santanu.maiti@saha.ac.in

1 Introduction

The sensitivity of electronic transport in low-dimensional systems like quantum dots [1, 2], mesoscopic loops [3, 4], quantum wires [5, 6], etc., on their geometry makes them truly unique in offering the possibility of electron transport in a very tunable way. These systems provide several anomalous characteristics in electron transport due to their reduced system dimensionality and quantum confinement. In the present age of nanoscience and technology, electronic devices made from quantum confined model systems are used extensively in fabrication of nano-electronic circuits where electron transport becomes predominantly coherent [7, 8]. The progress of theoretical description in a bridge system has been followed based on the pioneering work of Aviram and Ratner [9]. Later, the actual mechanisms underlying such transport become much more clearly resolved after several nice experimental observations [10, 11, 12] in different bridge systems. Though in literature many theoretical as well as experimental papers on electron transport are available, yet lot of controversies are still present between the theory and experiment, and the complete knowledge of the conduction mechanism in this scale is not very well established even today. Several key factors are there which control the electron transport across a bridge system, and all these effects have to be taken into account properly to characterize the transport. For our illustrative purposes, here we describe very briefly some of these factors. (I) The quantum interference effect [13, 14, 15, 16, 17] of electron waves passing through different arms of a conducting element which bridges two semi-infinite one-dimensional metallic electrodes, viz, source and drain becomes the most significant issue in electron transport in a bridge system. (II) The coupling of the electrodes with the bridging material provides an important signature in the determination of current amplitude [13]. The understanding of this coupling under non-equilibrium condition is a major challenge in this particular field, and we should take care about it in fabrication of any electronic device. (III) The geometry of the conducting material between the two electrodes itself is an important issue to control the electron transmission. To emphasize it, Emzerhof et al. [18] have predicted several model calculations and provided some new significant results. (IV) The dynamical fluctuation in the small-scale devices is another important factor which plays an active role and can be manifested

through the measurement of shot noise, a direct consequence of the quantization of charge [19, 20]. Beside these factors, several other parameters of the Hamiltonian that describe a system also provide significant effects in the determination of the current across a bridge system.

In the present paper, we will investigate the electron transport properties of a thin cylinder (see Fig. 1), attached to two semi-infinite one-dimensional metallic electrodes, in the presence of both longitudinal and transverse magnetic axes, μ_z and μ_y respectively. A simple tight-binding model is used to illustrate the system, where all the calculations are performed in the Green's function formalism. Our numerical study shows that, typical current amplitude across the cylinder oscillates as a function of the transverse magnetic axis μ_y , associated with the radial magnetic field B_r , showing N_0 flux-quantum periodicity instead of simple ϕ_0 -periodicity, where N and ϕ_0 ($= ch/e$) correspond to the size of the cylinder and the elementary flux-quantum respectively. This oscillatory behavior provides an important signature in this particular study. It is observed that, for a fixed bias voltage V applied by the electrodes, we can achieve a similar response for different cylinders by controlling the transverse magnetic axis associated with B_r . Thus, for the two cylinders of different sizes, similar response will be obtained for two different values of B_r , depending on the system size of the cylinder. For smaller cylinder, the response is obtained for lower value of B_r , while this similar response will be obtained for some higher value of B_r for the larger cylinder. This clearly manifests that a particular response can be delayed by tuning the system size N quite significantly. This aspect may be utilized in designing a tailor made switching device, and to the best of our knowledge, this phenomenon has not been addressed earlier in the literature.

We organize the paper as follows. Following the introduction (Section 1), in Section 2, we present the model and the theoretical formulations for our calculations. Section 3 discusses the significant results, and finally, we summarize our results in Section 4.

2 Model and the theoretical description

This section follows the methodology for the calculation of the transmission probability (T), conductance (g) and current (I) in a small cylinder by

using the Green's function technique.

We begin by referring to Fig. 1, where a cylinder is attached to two semi-infinite one-dimensional metallic electrodes, viz, source and drain. The cylinder is subjected to a longitudinal magnetic flux Φ_L , and a transverse magnetic flux Φ_t . For our illus-

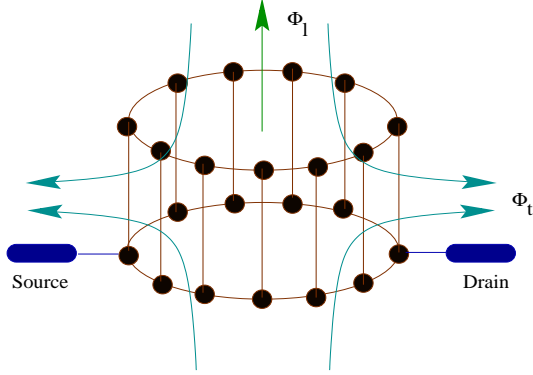


Figure 1: (Color online). Schematic view of a mesoscopic cylinder attached to two semi-infinite one-dimensional metallic electrodes and subjected to both the longitudinal and transverse magnetic fluxes Φ_L and Φ_t respectively. Filled circles correspond to the position of the atomic sites.

trative purpose here we consider the simplest possible cylinder, where only two isolated one-channel rings are connected by some vertical bonds. The transverse magnetic flux Φ_t is expressed in terms of the radial magnetic field B_r by the relation $\Phi_t = B_r L d$, where the symbols L and d correspond to the circumference of the ring and the height of the cylinder respectively.

At sufficient low temperature and bias voltage, we use the Landauer conductance formula [21, 22] to calculate the conductance g of the cylinder which can be expressed as,

$$g = \frac{2e^2}{h} T \quad (1)$$

where T becomes the transmission probability of an electron through the cylinder. It can be expressed in terms of the Green's function of the cylinder and its coupling to the two electrodes by the relation [21, 22],

$$T = \text{Tr} [S G_c^r D G_c^a] \quad (2)$$

where G_c^r and G_c^a are respectively the retarded and advanced Green's functions of the cylinder including the effects of the electrodes. The parameters S and D describe the coupling of the cylinder to the source and drain respectively, and they can

be defined in terms of their self-energies. For the complete system i.e., the cylinder with the two electrodes the Green's function is defined as,

$$G = (E - H)^{-1} \quad (3)$$

where $E = E + i\epsilon$. E is the injecting energy of the source electron and ϵ gives an infinitesimal imaginary part to E . Evaluation of this Green's function requires the inversion of an infinite matrix as the system consists of the infinite cylinder and the two semi-infinite electrodes. However, the entire system can be partitioned into sub-matrices corresponding to the individual sub-systems and the Green's function for the cylinder can be effectively written as,

$$G_c = (E - H_c - S - D)^{-1} \quad (4)$$

where H_c is the Hamiltonian of the cylinder which can be written in the tight-binding model within the non-interacting picture like,

$$\begin{aligned} H_c = & \sum_{i=1}^N \epsilon_i^L c_i^L c_i^L + \sum_{i=1}^N \epsilon_i^U c_i^U c_i^U \\ & + v_1^L \sum_{\langle ij \rangle} h_{ij} e^{i(\phi_1 - \phi_2)} c_i^L c_j^L + e^{-i(\phi_1 - \phi_2)} c_j^L c_i^L \\ & + v_1^U \sum_{\langle ij \rangle} h_{ij} e^{i(\phi_1 + \phi_2)} c_i^U c_j^U + e^{-i(\phi_1 + \phi_2)} c_j^U c_i^U \\ & + v_t \sum_{i=1}^N \epsilon_i^L c_i^L c_i^U + \epsilon_i^U c_i^U c_i^L \end{aligned} \quad (5)$$

In the above Hamiltonian (H_c), ϵ_i^L 's (ϵ_i^U 's) are the site energies in the lower (upper) ring, c_i^L (c_i^U) is the creation operator of an electron at site i in the lower (upper) ring, and the corresponding annihilation operator for this site i is denoted by c_i^L (c_i^U). The symbol v_1^L (v_1^U) gives the nearest-neighbor hopping integral in the lower (upper) ring, while the parameter v_t corresponds to the transverse hopping strength between the two rings of the cylinder. ϕ_1 and ϕ_2 are the two phase factors those are related to the longitudinal and transverse fluxes by the expressions, $\phi_1 = 2\pi \Phi_L / \Phi_0$ and $\phi_2 = 2\pi \Phi_t / \Phi_0$, where Φ_0 represents the total number of atomic sites in each ring and $\Phi_0 = ch/e$ is the elementary flux-quantum. Similar kind of tight-binding Hamiltonian is also used to describe the two semi-infinite one-dimensional perfect electrodes where the Hamiltonian is parametrized by constant on-site potential ϵ_0 and nearest-neighbor hopping integral t_0 . In Eq. 4, $S = h_{S_c}^\dagger g_S h_{S_c}$ and $D = h_{D_c}^\dagger g_D h_{D_c}$ are the self-energy operators due

to the two electrodes, where g_s and g_d correspond to the Green's functions of the source and drain respectively. h_{sc} and h_{dc} are the coupling matrices and they will be non-zero only for the adjacent points of the cylinder, and the electrodes respectively. The matrices s and d can be calculated through the expression,

$$s(d) = i \frac{h}{\epsilon} \frac{r}{s(d)} \frac{a}{s(d)} \quad (6)$$

where $\frac{r}{s(d)}$ and $\frac{a}{s(d)}$ are the retarded and advanced selfenergies respectively, and they are conjugate with each other. Datta et. al. [23] have shown that the selfenergies can be expressed like as,

$$\frac{r}{s(d)} = \frac{s(d)}{s(d)} - i \frac{s(d)}{s(d)} \quad (7)$$

where $\frac{s(d)}{s(d)}$ are the real parts of the selfenergies which correspond to the shift of the energy eigenvalues of the cylinder and the imaginary parts $\frac{s(d)}{s(d)}$ of the selfenergies represent the broadening of these energy levels. This broadening is much larger than the thermal broadening and this is why we restrict our all calculations only at absolute zero temperature. All the informations about the cylinder-to-electrode coupling are included into these two selfenergies.

The current passing across the cylinder is depicted as a single-electron scattering process between the two reservoirs of charge carriers. The current I can be computed as a function of the applied bias voltage V through the relation [21],

$$I(V) = \frac{e}{h} \int_{E_F - eV/2}^{E_F + eV/2} T(E; V) dE \quad (8)$$

where E_F is the equilibrium Fermi energy. For the sake of simplicity, we assume that the entire voltage is dropped across the cylinder-electrode interfaces and this assumption doesn't greatly affect the qualitative aspects of the I-V characteristics. Such an assumption is based on the fact that, the electric field inside the cylinder especially for small cylinders seems to have a minimal effect on the conductance-voltage characteristics. On the other hand, for quite larger cylinders and high bias voltages the electric field inside the cylinder may play a more significant role depending on the internal structure and size of the cylinder [23], yet the effect is quite small.

3 Results and discussion

To reveal the basic mechanisms of γ_1 and γ_t on the electron transport, here we present all the results

only for the non-interacting electron picture. With this assumption, the model becomes quite simple and all the basic features can be well understood. Another realistic assumption is that, we focus on the perfect cylinders only i.e., the site energies are taken as $\epsilon_i^L = \epsilon_i^U = 0$ for all i . As illustrative purposes, we parameterize all the hopping integrals (v_1^L , v_1^U and v_t) of the cylinder by a single parameter v , viz, we set $v_1^L = v_1^U = v_t = v$. In the present article, we concentrate our study of electron transport in the two separate regimes. These are so-called

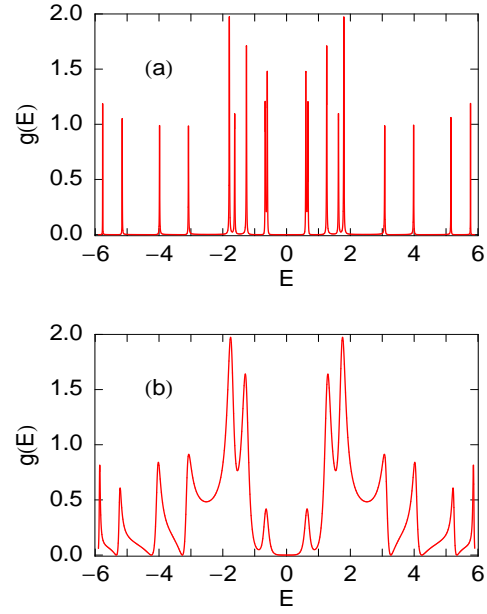


Figure 2: (Color online). g - E characteristics for a thin cylinder with $N = 12$, $\gamma_1 = 0.2$ and $\gamma_t = 2$. (a) weak-coupling limit and (b) strong-coupling limit.

the weak-coupling and strong-coupling regimes respectively. The weak-coupling regime is specified by the condition $\gamma_{s,d} < v$. On the other hand, the condition $\gamma_{s,d} > v$ is used to denote the strong-coupling regime. Here, the parameters s and d correspond to the hopping strengths of the cylinder to the source and drain respectively. In these two limiting cases, we choose the values of the different parameters as follow: $s = d = 0.5$, $v = 2.5$ (weak-coupling) and $s = d = 2$, $v = 2.5$ (strong-coupling). The on-site energy ϵ_0 is set to 0 (we can take any constant value of it instead of zero, since it provides only the reference energy level) for the electrodes, and the hopping strength t_0 is taken as 3 in the two semi-infinite metallic electrodes. For the sake of simplicity, we set the Fermi energy $E_F = 0$

and choose the units where $c = e = h = 1$.

Let us begin our discussion with the variation of the conductance g as a function of the injecting electron energy E . As illustrative examples, in Fig. 2 we plot the conductance-energy (g - E) characteristics for a thin cylinder with $N = 12$, considering the parameters $\gamma_1 = 0.2$ and $\gamma_t = 2$. Figures 2(a) and (b) correspond to the results for the weak- and strong-coupling regimes respectively. It shows that, in the limit of weak-coupling, the conductance exhibits resonance peaks for some particular energies, while for all other energies the conductance almost disappears. Out of these resonance peaks, only for the two energies the conductance approaches the value 2. Thus, for these energies the transmission probability T becomes unity, since we

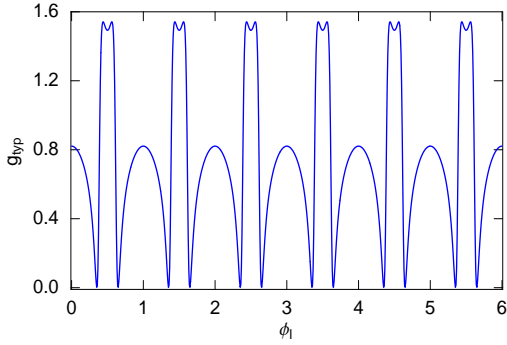


Figure 3: (Color online). Typical conductance as a function of ϕ_1 for a thin cylinder with $N = 12$ in the strong-coupling limit, where the parameter γ_t is set to 2. The conductance is calculated at the energy $E = 2.1$.

get the relation $g = 2T$ from the Landauer conductance formula (see Eq. 1 with $e = h = 1$). On the other hand, for other resonances, the conductance does not reach to 2 any more, and gets much reduced value. This is due to the quantum interference effect of the electronic waves passing through the different arms of the cylinder, and it can be interpreted as follows. During the motion of the electrons from the source to drain through the cylinder, the electron waves propagating along the different possible pathways can get a phase shift among them selves, according to the result of quantum interference. Therefore, the probability amplitude of getting an electron across the cylinder either becomes strengthened or weakened. This causes the transmittance cancellations and provides anti-resonances in the conductance spectrum. Thus it can be emphasized that the electron transmission is strongly affected by the quantum interference ef-

fects, and hence the cylinder to electrodes interface structure. Now all these resonance peaks are associated with the energy eigenvalues of the cylinder, and accordingly, we can say that the conductance spectrum manifests itself the electronic structure of the cylinder. In the resonance spectrum we get more peaks in the presence of both γ_1 and γ_t compared to those as obtained when both these two axes are identically zero. This is due to the fact that the axes γ_1 and γ_t remove all the degenera-

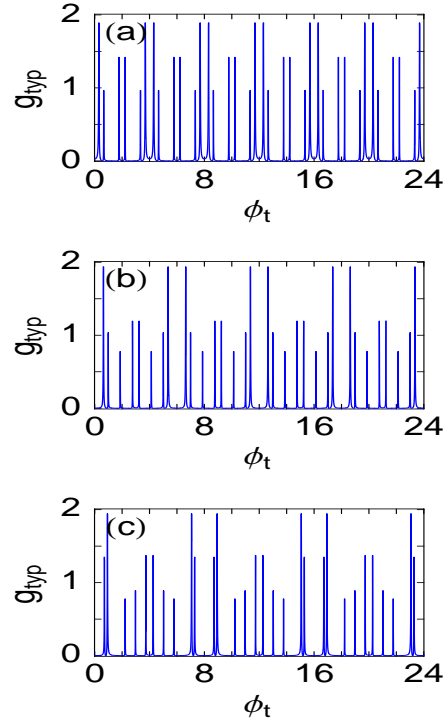


Figure 4: (Color online). Typical conductances as a function of ϕ_t for three different cylinders with (a) $N = 4$, (b) $N = 6$ and (c) $N = 8$ respectively, in the limit of weak-coupling. The energy E is fixed at 2.1 and the parameter γ_1 is set to 0.2.

cies in the energy levels which provide more resonance peaks in the conductance spectrum. With these features, we get additional one feature when the coupling strength of the cylinder to the electrodes increases from the low regime to high one. In the limit of strong cylinder-to-electrode coupling, all these resonances get substantial widths compared to the weak-coupling limit. The results are shown in Fig. 2(b). The contribution for the broadening of the resonance peaks in this strong-coupling limit appears from the imaginary parts of the self-energies Σ_S and Σ_D respectively [21], as mentioned

earlier. Thus by tuning the coupling strength, we can get the electron transmission across the cylinder for wider range of energies and it provides an important signature in the study of current-voltage characteristics.

In order to express the dependence of both the two different axes on the electron transport much more clearly, in Figs. 3 and 4 we display the variation of the typical conductances as a function of ϕ_1 and ϕ_t respectively. Figure 3 shows the variation of the typical conductance (g_{typ}) with the longitudinal magnetic flux ϕ_1 in the limit of strong-coupling for a cylinder considering $N = 12$. Here we calculate

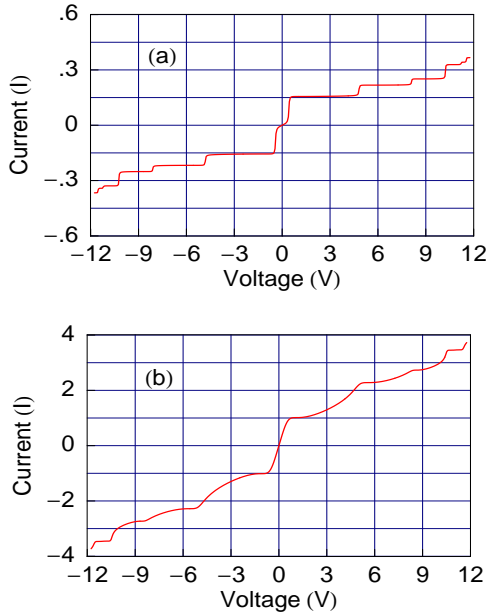


Figure 5: (Color online). I-V characteristics for a thin cylinder with $N = 6$, $\phi_1 = 0.2$ and $\phi_t = 2$. (a) weak-coupling limit and (b) strong-coupling limit.

g_{typ} for the energy $E = 2.1$, when the parameter ϕ_t is set to 2. It shows that the typical conductance exhibits oscillatory behavior with ϕ_1 showing ϕ_0 ($= 1$, since $c = e = h = 1$ in our present formulation) flux-quantum periodicity. This ϕ_0 periodicity is well known in the literature. The remarkable behavior is observed only for the case when we apply the transverse magnetic flux in the cylinder. For the illustrative purposes, in Fig. 4 we plot the variation of the typical conductance of the three different cylinders in the limit of weak-coupling, where (a), (b) and (c) correspond to the results for the cylinders with $N = 4, 6$ and 8 respectively. In this case, we set the energy $E = 2.1$ and ϕ_1 to 0.2 . Quite

interestingly it is observed that, the typical conductance varies periodically with the flux ϕ_t showing $N \phi_0$ flux-quantum periodicity, instead of the traditional ϕ_0 flux-quantum periodicity as observed in the previous case. The detailed investigation reveals that the nature of the g_{typ} vs. ϕ_t characteristic within a single period of any one of these three cylinders is quite similar to that of the other two cylinders within their respective periods. Thus the positions of the resonance peaks shift appropriately with the increase of the system size N to make the nature invariant. This is really a very interesting phenomenon and can be utilized to get a delayed response just by tuning the system size N .

All these features of electron transport become much more clearly visible by studying the current-voltage (I-V) characteristics. The current across

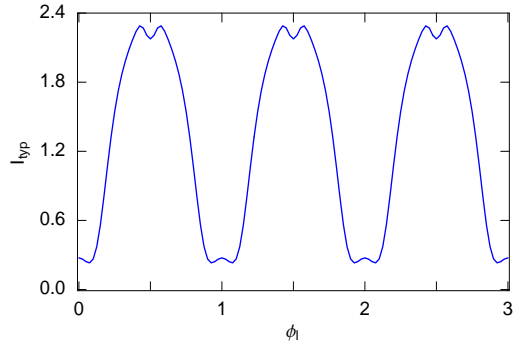


Figure 6: (Color online). Typical current amplitude as a function of ϕ_1 for a thin cylinder with $N = 6$ in the strong-coupling limit, where the parameter ϕ_t is set to 2. The current is calculated at the bias voltage $V = 1.95$.

the cylinder is computed from the integration procedure of the transmission function T as prescribed in Eq. 8. The transmission function varies exactly similar to that of the conductance spectrum, differ only in magnitude by the factor 2 since the relation $g = 2T$ holds from the Landauer conductance formula Eq. 1. As representative examples, in Fig. 5 we plot the current-voltage characteristics for a thin cylinder with $N = 6$, $\phi_1 = 0.2$ and $\phi_t = 2$, where (a) and (b) represent the results for the weak and strong cylinder-to-electrode coupling limits respectively. In the limit of weak-coupling, the current exhibits staircase-like structure with the steps as a function of the applied bias voltage. This is due to the existence of the sharp resonance peaks in the conductance spectrum in this limit of coupling, since the current is computed by the integration method of the transmission function T . With

the increase of the applied bias voltage, the electrochemical potentials on the electrodes are shifted gradually, and finally cross one of the quantized energy levels of the cylinder. Accordingly, a current channel is opened up and the current-voltage characteristic curve provides a jump. On the other hand, for the strong cylinder-to-electrode coupling, the current varies almost continuously with the applied bias voltage and achieves much larger amplitude than the weak-coupling case. The reason is that, in the limit of strong-coupling all the energy levels get broadened which provide larger current in

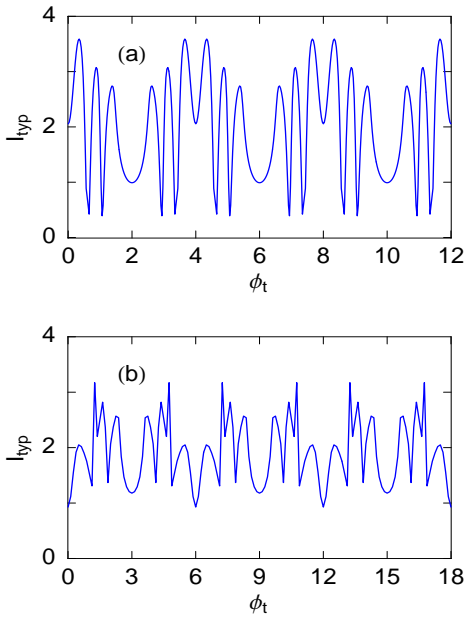


Figure 7: (Color online). Typical current amplitudes as a function of ϕ_t for two different cylinders with (a) $N = 4$ and (b) $N = 6$ respectively, in the limit of strong-coupling. The voltage V is fixed at 0.7 and the parameter γ_1 is set to 0.3.

the integration procedure of the transmission function T . Thus by tuning the strength of the cylinder-to-electrode coupling, we can achieve very large current amplitude from the very low one for the same bias voltage V .

Finally, we concentrate our study on the variation of the typical current amplitude (I_{typ}) with the magnetic fluxes γ_1 and ϕ_t to illuminate the significant effects of these fluxes on the electron transport. In Fig. 6, we display the variation of I_{typ} as a function of γ_1 for a thin cylinder with $N = 6$ in the limit of strong-coupling, where the parameter ϕ_t is fixed to 2. The typical current is computed at the bias

voltage $V = 1.95$. It predicts that the current amplitude shows an oscillatory behavior with γ_1 , giving ϕ_0 -flux-quantum periodicity. This is completely analogous to the variation of g_{typ} with γ_1 as described earlier. The interesting feature is observed only when we study the variation of I_{typ} with ϕ_t , instead of γ_1 . The results are shown in Fig. 7, where (a) and (b) correspond to the variation of the current amplitudes for the cylinders with $N = 4$ and 6 respectively. The typical current amplitudes are calculated in the limit of strong-coupling for the bias voltage $V = 0.7$, when the parameter γ_1 is set to 0.3. Quite interestingly we see that, the current amplitude varies periodically with ϕ_t providing $N \phi_0$ -flux-quantum periodicity, instead of the conventional ϕ_0 periodicity. Thus for the cylinder with $N = 4$, the current shows 4 ϕ_0 ($= 4$) periodicity, while it becomes 6 ϕ_0 ($= 6$) for the cylinder with $N = 6$. From these results we clearly observe that the variation of I_{typ} with ϕ_t within a period for the cylinder with $N = 6$ is quite similar to that of the cylinder with $N = 4$ within its single period. This is just the replica of the g_{typ} versus ϕ_t characteristics which we have described earlier. Thus for a fixed bias voltage, we can achieve the similar response for different values of N just by tuning the flux ϕ_t associated with the radial magnetic field B_r . This phenomenon can be utilized as follows. Let us consider two such cylinders of different sizes. For these two cylinders, a particular response is obtained for the two different values of B_r , depending on the size of these cylinders. Therefore, for the cylinder of smaller size the similar response is achieved at the lower value of B_r compared to the cylinder of larger size. This clearly manifests that a particular response can be delayed by tuning the size N of the cylinder quite significantly. This aspect is really a very interesting, and provides a signature for manufacturing mesoscopic switching devices.

4 Concluding remarks

In conclusion, we have addressed the electron transport in a thin cylinder, attached to two semi-infinite one-dimensional metallic electrodes, in the presence of both longitudinal and transverse magnetic fluxes. We have used a simple tight-binding model to describe the system where all the calculations have been done in the Green's function formalism. Quite interestingly we have observed that the typical current amplitude oscillates as a function of the transverse magnetic flux ϕ_t , associated with the conductance-energy characteristics, providing

N_0 ux-quantum periodicity. This feature is completely different from the traditional oscillatory behavior like as we have got for the case of I_{typ} versus μ_1 characteristic. Our results have predicted that a particular response can be delayed by tuning the size of the cylinder N . This aspect may be utilized in designing a tailor made mesoscopic switching device.

This is our first step to describe how the electron transport in a thin cylinder can be controlled very nicely by means of the longitudinal and transverse magnetic axes. We have made several realistic assumptions by ignoring the effects of the electron-electron correlation, disorder, temperature, finite width of the electrodes, etc. Here we discuss very briefly about these approximations. The inclusion of the electron-electron correlation in the present model is a major challenge to us, since over the last few years many people have studied a lot to incorporate this effect, but no such proper theory has yet been developed. In this work, we have presented all the results only for the ordered systems. But in real samples, the presence of impurities will affect the electronic structure and hence the transport properties. The effect of the temperature has already been pointed out earlier, and, it has been examined that the presented results will not change significantly even at finite temperature, since the broadening of the energy levels of the cylinder due to its coupling with the electrodes will be much larger than that of the thermal broadening [21]. The other important assumption is that here we have chosen the linear chains instead of wider leads, since we are mainly interested about the basic physics of the cylinder. Though the results presented here change with the increase of the thickness of the leads, but all the basic features remain quite invariant. Finally, we would like to say that we need further study in this system by incorporating all these effects.

Acknowledgments

I acknowledge with deep sense of gratitude the illuminating comments and suggestions I have received from Prof. Arunava Chakrabarti and Prof. S. N. Karmakar during the calculations.

References

[1] S. M. Cronenwett, T. H. Oosterkamp, L. P. Kouwenhoven, *Science* 281 (1998) 5.

[2] A. W. Holleitner, R. H. Blick, A. K. Huttel, K. Eber, J. P. Kotthaus, *Science* 297 (2002) 70.

[3] I. O. Kulik, *Physica B* 284 (2000) 1880.

[4] I. O. Kulik, *JETP Lett.* 11 (1970) 275.

[5] P. A. Orellana, M. L. Ladrón de Guevara, M. Pacheco, A. Latge, *Phys. Rev. B* 68 (2003) 195321.

[6] P. A. Orellana, F. Domínguez-Adame, I. Gómez, M. L. Ladrón de Guevara, *Phys. Rev. B* 67 (2003) 085321.

[7] A. Nitzan, *Annu. Rev. Phys. Chem.* 52 (2001) 681.

[8] A. Nitzan, M. A. Ratner, *Science* 300 (2003) 1384.

[9] A. Aviram, M. Ratner, *Chem. Phys. Lett.* 29 (1974) 277.

[10] T. Dadoosh, Y. Gordin, R. Krahne, I. Khivrich, D. Mahali, V. Frydman, J. Sperling, A. Yacoby, I. Bar-Joseph, *Nature* 436 (2005) 677.

[11] J. Chen, M. A. Reed, A. M. Rawlett, J. M. Tour, *Science* 286 (1999) 1550.

[12] M. A. Reed, C. Zhou, C. J. Muller, T. P. Burgin, J. M. Tour, *Science* 278 (1997) 252.

[13] R. Baer, D. Neuhauser, *Chem. Phys.* 281 (2002) 353.

[14] R. Baer, D. Neuhauser, *J. Am. Chem. Soc.* 124 (2002) 4200.

[15] D. Walter, D. Neuhauser, R. Baer, *Chem. Phys.* 299 (2004) 139.

[16] K. Tagami, L. Wang, M. Tsukada, *Nano Lett.* 4 (2004) 209.

[17] K. Walczak, *Cent. Eur. J. Chem.* 2 (2004) 524.

[18] M. Emzerhof, M. Zhuang, P. Rocheleau, J. Chem. Phys. 123 (2005) 134704.

[19] Y. M. Blanter, M. Buttiker, *Phys. Rep.* 336 (2000) 1.

[20] K. Walczak, *Phys. Stat. Sol. (b)* 241 (2004) 2555.

[21] S. Datta, *Electronic transport in mesoscopic systems*, Cambridge University Press, Cambridge (1997).

- [22] M . B . Nardelli, Phys. Rev. B 60 (1999) 7828.
- [23] W . T ian, S . Datta, S . Hong, R . Reifengerger,
J . I . Henderson, C . I . Kubiak, J . Chem . Phys.
109 (1998) 2874.